atmosphere

MDPI

Article

Relative Humidity Impact on Organic New Particle Formation from Ozonolysis of α- and β-Pinene at Atmospherically Relevant Mixing Ratios

Christopher N. Snyder, Austin C. Flueckiger and Giuseppe A. Petrucci *

Department of Chemistry, University of Vermont, Burlington, VT 05405, USA
* Correspondence: giuseppe.petrucci@uvm.edu

Abstract: The impact of relative humidity (RH) on organic new particle formation (NPF) from ozonolysis of monoterpenes remains an area of active debate. Previous reports provide contradictory results indicating both depression and enhancement of NPF under conditions of moderate RH, while others do not indicate a potential impact. Only several reports have suggested that the effect may depend on absolute mixing ratio of the precursor volatile organic compound (VOC, ppb_v). Herein we report on the impact of RH on NPF from dark ozonolysis of α- and β-pinene at mixing ratios ranging from 0.2 to 80 ppb_v. We show that RH enhances NPF (by a factor of eight) at the lowest α-pinene mixing ratio, with a very strong dependence on α-pinene mixing ratio from 4 to 22 ppb_v. At higher mixing ratios, the effect of RH plateaus, with resulting modest decreases in NPF. In the case of α- and β-pinene, NPF is enhanced at low mixing ratios due to a combination of chemistry, accelerated kinetics, and reduced partitioning of semi-volatile oxidation products to the particulate phase. Reduced partitioning would limit particle growth, permitting increased gas-phase concentrations of semi- and low-volatility products, which could favor NPF.

Keywords: α-pinene; secondary organic aerosol; relative humidity; new particle formation

Citation: Snyder, C.N.; Flueckiger, A.C.; Petrucci, G.A. Relative Humidity Impact on Organic New Particle Formation from Ozonolysis of α- and β-Pinene at Atmospherically Relevant Mixing Ratios. *Atmosphere* **2023**, *14*, 173. https://doi.org/10.3390/atmos14010173

Academic Editors: Xiao Sui and Houfeng Liu

Received: 23 November 2022
Revised: 6 January 2023
Accepted: 10 January 2023
Published: 13 January 2023

1. Introduction

It is well accepted that the oxidation of volatile organic compounds (VOCs) in the atmosphere contributes significantly to secondary organic aerosol (SOA) formation. Some estimates place the fraction of SOA mass in organic aerosol (OA) fine and ultrafine particles in continental air masses to be greater than 70% [1]. Monoterpenes are a major contributor to atmospheric SOA by way of oxidation with numerous atmospheric gases to form low volatility compounds that either form new particles or partition to existing particles [1–3]. One of the most studied monoterpenes to date is α-pinene, a C-10 unsaturated VOC, emitted by a variety of terrestrial vegetation and other sources [4,5]. Typical biogenic emissions are in the parts-per-trillion by volume range, with episodic events (especially in warmer months) producing as much as 50–60 ppb_v of monoterpenes [5–8]. Many questions remain, however, concerning operational oxidation mechanisms for α-pinene ozonolysis that lead to the formation of SOA and, more specifically, new particle formation (NPF). Herein we define SOA exclusively as the mass loading of OA, whereas NPF refers exclusively to the particle number density. Some uncertainty in our understanding of SOA formation is likely from conflicting studies regarding the impact of relative humidity (RH) on NPF and SOA formation from the ozonolysis of terpenes such as α- and β-pinene.

The majority of studies to date have been conducted at fixed and uncharacteristically low levels of RH that are not representative of the lower troposphere [9], where most NPF and SOA formations are hypothesized to occur. A few studies have been reported to better understand the role of RH in NPF and SOA generation from α-pinene ozonolysis. These results have been contradictory, with some reporting an enhancement in NPF and/or SOA as a result of higher RH [10–13], while others report a sharp reduction [11,14–19]. It remains

unclear what might be causing discrepancies in reported results. Further exacerbating the issue are the very different VOC and oxidant mixing ratios (ξ_{VOC}, ppb_v) used in laboratory studies, which have ranged from parts-per-trillion by volume ($pptr_v$) to parts-per-million by volume (ppm_v), the latter predominantly in studies employing flow reactors with short reaction times of up to a few minutes. It is unlikely that results obtained at these high VOC/ozone mixing ratios are representative of the natural environment, and may be providing inaccurate data and guidance to atmospheric models. For example, preliminary, qualitative experiments in our laboratory conducted at VOC mixing ratios similar to previous studies reported in the literature (for example, [12,20,21]) support a decrease in SOA and NPF at high RH. However, these same experiments conducted at VOC mixing ratios closer to atmospheric relevance suggest, instead, a potential enhancement in NPF at high RH.

Herein, we report on the impact of RH on NPF and SOA from the dark ozonolysis of α- and β-pinene in an environmental chamber at mixing ratios of 0.2 to 80 ppb_v. We show that RH impacts NPF in a nonlinear manner and that the correlation of NPF with RH could be positive or negative as a function of ξ_{VOC}. Results suggest that the point of inflection, at least for these two monoterpenes, between enhancement and suppression of NPF may depend on the SOA-forming potential of the VOC.

2. Materials and Methods

2.1. Experimental Conditions

All experiments were conducted with α-pinene (Alfa Aesar, Haverhill, MA, USA, 98%, CAS: 7785-70-8) and β-pinene (Sigma Aldrich, St. Louis, MO, USA, 99%, CAS: 19902-08-0) without further purification. Ozone was generated with a commercial unit by passage of dry, particle-free air through a corona discharge (Ozone Technologies LLC, Model 1KNT, Jersey City, NJ, USA). Ozone was injected by diverting the output flow of the generator to the chamber for a pre-determined time pulse to yield the desired ozone concentration. Typical injection pulses were in the range of 10–120 s, depending on the size of the chamber in use. Ozone concentrations in the chambers were monitored continuously (Serinus 10, American Ecotech, Warren, RI, USA).

Two Teflon reaction chambers were utilized separately for this work and are referred to as the 775 L Particle Genesis Chamber (PGC) and the 8 m^3 University of Vermont Environmental Chamber (UVMEC) [22]. For both types of reaction chambers, zero air was used for flushing until background aerosol mass and number concentrations were below 0.01 μg m^{-3} and 10 particles cm^{-3}, respectively. A glass micro-syringe was used to quantitatively transfer α-pinene aliquots into a glass three-neck flask that was placed in a hot water bath. The liquid phase α-pinene content within the flask was visually monitored as a 200 mL min^{-1} flow of zero-air carried the volatilized α-pinene into the reaction chamber. Once all α-pinene was introduced, the zero-air flow was shut off after 10–20 min of continuous flow. All experiments were conducted under ambient temperature and atmospheric pressure. Following each experiment, an injection of hydrogen peroxide (30%, Fisher Scientific, CAS: 7722-84-1) was used to passivate the chamber with UV lights overnight.

Particle metrics (number, mass, and size distributions) were measured using a scanning mobility particle sizer (SMPS 3082, TSI Inc., Shoreview, MN, USA) operating with sheath and aerosol flows of 10 and 1.0 L min^{-1}, respectively. Rates of NPF were determined using an electrical low-pressure impactor (ELPI+, Dekati Technologies Ltd., Kangasala, Finland).

Experimental details for experiments studying NPF as a function of RH and ξ_{VOC} are summarized in Table 1. SOA mass loading (C_{SOA}) values obtained from SMPS measurements have been corrected for wall losses using ammonium sulfate in accordance with a previously established method [23]. All experiments were conducted at least in duplicate and with ξ_{O3} = 500 ppb_v. Experiments aP_6RH_0 and aP_6RH_{60} were repeated four times each to estimate a typical measurement error.

Table 1. Parameters for all NPF chamber experiments reported herein pertaining to α-pinene. In all cases, chamber temperature was 20 (±1) °C.

Experiment	ξ_{VOC} (ppb_v)	RH (%)
aP_4RH_0/RH_{60}	4	0/60
aP_6RH_0/RH_{60}	6	0/60
$aP_{10}RH_0/RH_{60}$	10	0/60
$aP_{22}RH_0/RH_{60}$	22	0/60
$aP_{50}RH_0/RH_{60}$	50	0/60
$aP_{66}RH_0/RH_{60}$	66	0/60
$aP_{80}RH_0/RH_{60}$	80	0/60

2.2. Measurement of NPF Rates

A series of varying RH experiments were carried out to probe the kinetics of NPF enhancement under elevated RH for the ozonolysis of α-pinene at atmospherically relevant ξ_{VOC} (Table 2). All NPF rate experiments were conducted in the UVMEC with ξ_{O3} = 500 ppb_v at ambient temperature (20 ± 1 °C) and atmospheric pressure. For this experimental set, an optimized injection setup was used for VOC delivery [24]. In summary, a ball valve was used on the injection setup inlet to deliver one pulse of zero air for gas-phase injection of the VOC in its entirety. A tunable split valve was implemented on the injection setup outlet for increased VOC injection volumes. The zero-air flow rate to the UVMEC was 2.0 ± 0.1 L min^{-1}. The ELPI+ data output was a summation of the particle number in all size bins (# cm^{-3} s^{-1}, 14 bins, 6 nm–15 μm). The slope of the extracted particle number curve was normalized for rate comparison at varying RH.

Table 2. Parameters for all rate of NPF UVMEC experiments reported herein. n = 1 for each RH.

Experiment	ξ_{VOC} (ppb_v)	RH (%)
$aP_{10}RH_0$	9.9	0.0
$aP_{10}RH_8$	9.8	8.0
$aP_{10}RH_{16}$	10.0	16.0
$aP_{10}RH_{30}$	10.1	30.0
$aP_{10}RH_{60}$	10.0	60.6

3. Results

Previous experiments in our laboratory have suggested, albeit in a qualitative manner, that elevated RH may produce enhanced NPF and SOA from the dark ozonolysis of terpenes, such as α- and β-pinene (Figure 1). Therefore, this report describes an extension of these preliminary results by undertaking systematic chamber experiments to quantitatively probe the role of RH on NPF and SOA generation from dark ozonolysis of α- and β-pinene at ξ_{VOC} of 0.2 to 80 ppb_v. Table 3 summarizes absolute particle number densities obtained for various ξ_{VOC} at dry (0%) and high (60%) RH. As shown in Figure 2, we see general agreement between dry and humid conditions at elevated ξ_{VOC}, but a rather dramatic divergence in NPF as a function of RH at lower, more atmospherically relevant ξ_{VOC}. Somewhat surprisingly, SOA mass loading was greater under elevated RH for all ξ_{VOC} studied.

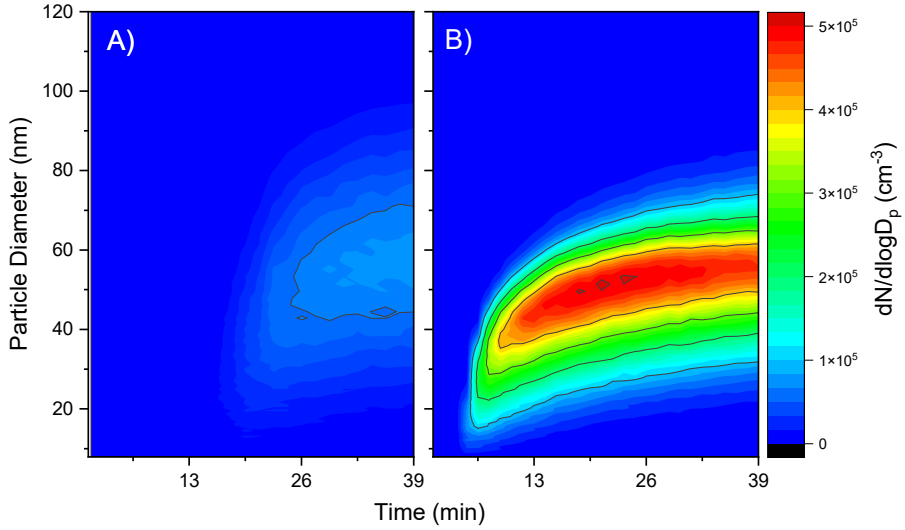

Figure 1. Evolution of OA particle size distributions for dark ozonolysis of 6-ppb$_v$ α-pinene under (**A**) dry (<1%RH) and (**B**) humid (60%RH) conditions. ξ_{O3} = 500 ppb$_v$.

Table 3. Parameters for all chamber experiments reported herein pertaining to α-pinene. In all cases, chamber temperature was 20 ($\pm$1) °C. N_{max} and $C_{SOA,max}$ are the maximum number of particles and SOA mass, respectively, formed in the experiment. Note: error bounds were estimated based on replicate (n = 4) measurements made in experiments aP_6RH_0 and aP_6RH_{60}.

Experiment	N_{max} (Dry, cm^{-3})	N_{max} (Humid, cm^{-3})	ΔN_{max}	$C_{SOA,max}$ (μg m^{-3})	$\Delta C_{SOA,max}$
aP_4RH_0/RH_{60}	8.51×10^3	7.51×10^4	7.8	3.97/6.41	0.61
aP_6RH_0/RH_{60}	2.57×10^4	1.44×10^5	5.7	3.5/11.5	2.3
$aP_{10}RH_0/RH_{60}$	6.10×10^4	2.13×10^5	1.8	11/17	0.55
$aP_{22}RH_0/RH_{60}$	1.05×10^5	2.20×10^5	0.51	14/27	0.93
$aP_{50}RH_0/RH_{60}$	2.10×10^5	1.69×10^5	−0.20	85/109	0.22
$aP_{66}RH_0/RH_{60}$	1.85×10^5	2.36×10^5	0.28	56/75	0.34
$aP_{80}RH_0/RH_{60}$	3.70×10^5	2.90×10^5	−0.21	124/119	−0.04

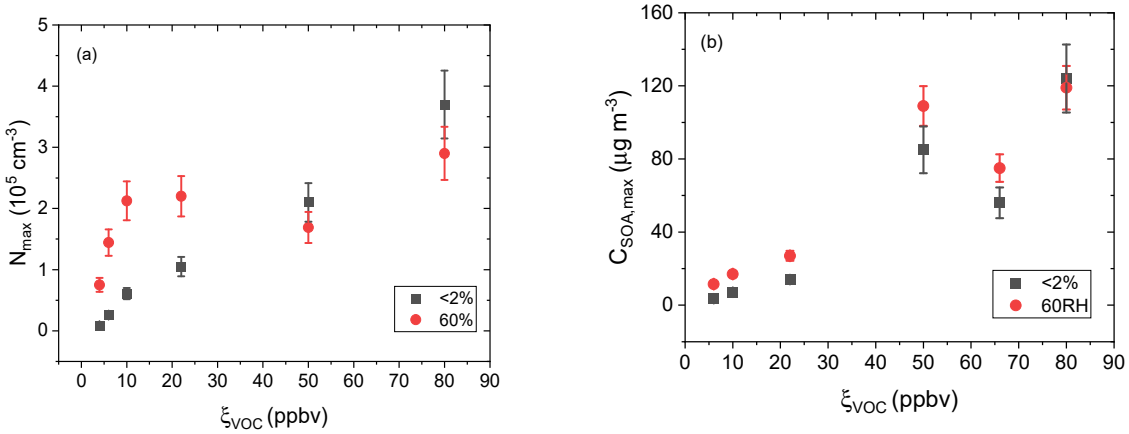

Figure 2. Maximum (**a**) number density (N_{max}) and (**b**) SOA mass obtained from ozonolysis of α-pinene at (■) <2% and (●) 60% RH as a function of ξ_{VOC}. Relative standard deviation (n = 4), measured experimentally for experiments aP_6RH_0 and aP_6RH_{60}, was applied to all other experimental measures.

A quantitative representation of RH impacts on NPF under humid conditions is afforded by the parameter ΔN_{max}, which is calculated according to Equation (1) relative to dry conditions:

$$\Delta N_{max} = \frac{N_{max(60RH)} - N_{max(0RH)}}{N_{max(0RH)}} \quad (1)$$

ΔN_{max} has a minimum value of −1 for complete elimination of NPF by RH, but no upper bound. Interestingly, we see that at low ξ_{VOC}, high RH results in increased NPF (Figure 3) in a non-linear fashion. However, at higher ξ_{VOC} of about 50 ppb_v, the trend inverts, with high RH suppressing NPF, in accord with previous results [21]. Figure 3 highlights the absolute magnitude of the NPF enhancement, placing it in relation to the NPF observed for those same mixing ratios under dry conditions. Furthermore, it permits comparisons with the existing literature. For the latter cases, number data were obtained directly from tables in the previous reports or interpolated from graphical data. Using the absolute maximum particle number densities from the other reports in conjunction with Equation (1) allows us to estimate their NPF enhancement as a function of RH even though their O_3 mixing ratios were somewhat lower than used in the present study, and different environmental chambers/flow reactors were used.

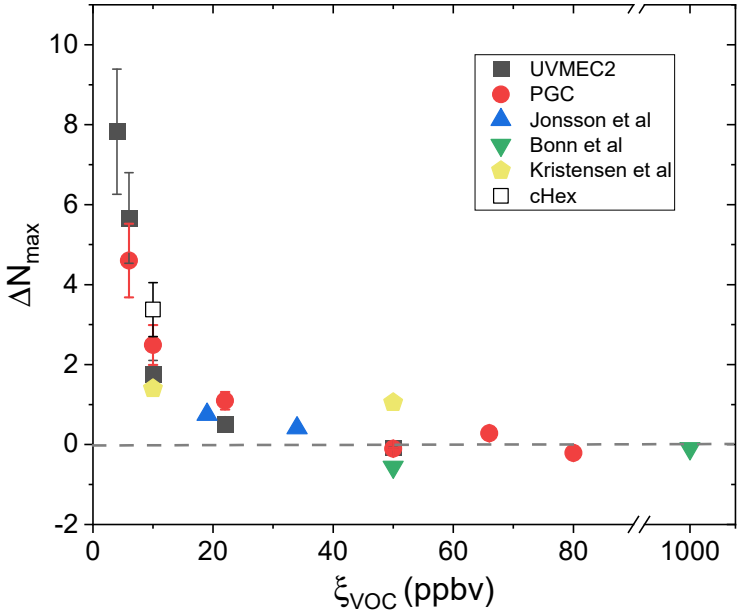

Figure 3. Change in maximum number of particles formed by ozonolysis of α-pinene at different ξ_{VOC}. N_{60} and N_0 are the maximum number of particles formed at RH = 60% and 0%, respectively. ΔN = −1 for the case of complete shutdown of NPF and ΔN = 0 for no change. Dashed line represents ΔN if water had no impact on NPF. UVMEC: University of Vermont Environmental Chamber (8 m^3); PGC: particle genesis chamber (0.4 m^3); cHex: cyclohexane as OH scrubber added at a VOC:cHex mole ratio of 1:100; The literature values are inferred from Jonsson et al. [12,25], Bonn et al. [21], and Kristensen et al. [26].

A similar trend was observed for dry SOA mass (as measured with the SMPS) produced under dry and humid conditions (Figure 4). Since the recirculating sheath air in the SMPS remained at RH < 30% for the duration of any single experiment, any liquid water taken up by organic particles in the reaction chamber should quickly evaporate during size measurement. We confirmed that SOA size distributions measured at high RH in the chamber were, in fact, for dried particles by comparing particle size distributions pre- and post-passage through a 30-cm long diffusion drier. No difference in size distribution was measured, suggesting that the SOA particles measured with the SMPS are "fully dried", and that measured increases in C_{SOA} correspond only to organic material.

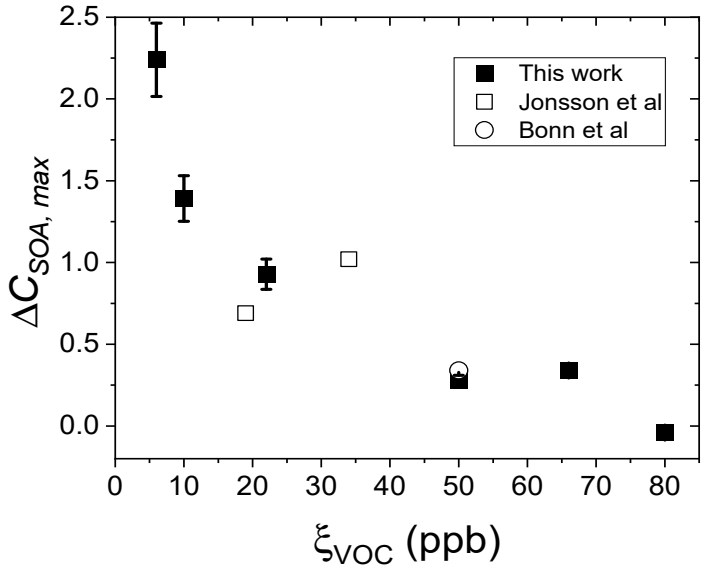

Figure 4. Change in dry SOA mass formed by ozonolysis of α-pinene at different ξ_{VOC}. ΔN = −1 for the case of complete shutdown of SOA formation and ΔN = 0 for no change. Error bars indicate one standard deviation for n = 4. The literature values are inferred from Jonsson et al. [12,25] and Bonn et al. [21].

At high RH, a greater number of smaller particles were formed, with modest increases in $\Delta C_{SOA,\,max}$ as a function of decreasing ξ_{VOC}. While the enhanced NPF at high RH and low ξ_{VOC} likely drives the majority of the increased SOA mass, a contribution could also made due to enhanced partitioning of semi-volatile and low volatile organic compounds (S- and L-VOCs) to the particle phase driven by increased SOA phase water in the reaction chamber at high RH. Increased liquid water content will drive down the average molecular weight of the organic matter, thereby favoring SOA condensation [27,28]. While contribution of this mechanism to SOA growth is considered modest [29], it may depend strongly on particle phase [30].

3.1. Comparison to the Literature Reports

Studies typically indicate a negative correlation between RH and NPF. However, closer inspection of NPF and SOA formation data at the lower range of ξ_{VOC} studied suggests that this may not be the case. For example, Emanuelsson et al. [11] reported NPF for ozonolysis of β-pinene as a function of RH for three VOC mixing ratios: 79, 109, and 164 ppb_v. In all cases, a decrease in NPF was measured (Figure 5a, extrapolated from data reported [11]). Considering only RH < 30% (below which there appears to be an inverse linear relationship between N_{max} and RH), the slope from the linear regression for each data set can be plotted as a function of ξ_{VOC} to yield a linear curve with a y-intercept of 0.56 (Figure 5b). This suggests that, at low ξ_{VOC}, there could exist a positive correlation between N_{max} and RH. We therefore conducted analogous experiments in the UVMEC with β-pinene at two RHs: <1% and 30%. The results are presented in Figure 6. As predicted from the data of Emanuelsson et al. [11], we see a reduction in NPF between the dry and humid trials at elevated ξ_{VOC} that inverts at about ξ_{VOC} = 0.5 ppb_v. At ξ_{VOC} = 0.2 ppb_v, while the absolute numbers of particles under dry and humid conditions decrease, as one would expect for the lower mixing ratio, we see a significant enhancement in NPF for the humid trial as compared to the dry trial. Note that the ξ_{VOC} used in this work cannot be compared directly to that of Emanuelsson et al. [11], as their experiments were conducted in a flow tube reactor, which requires much higher reactant mixing ratios due to the short reaction times.

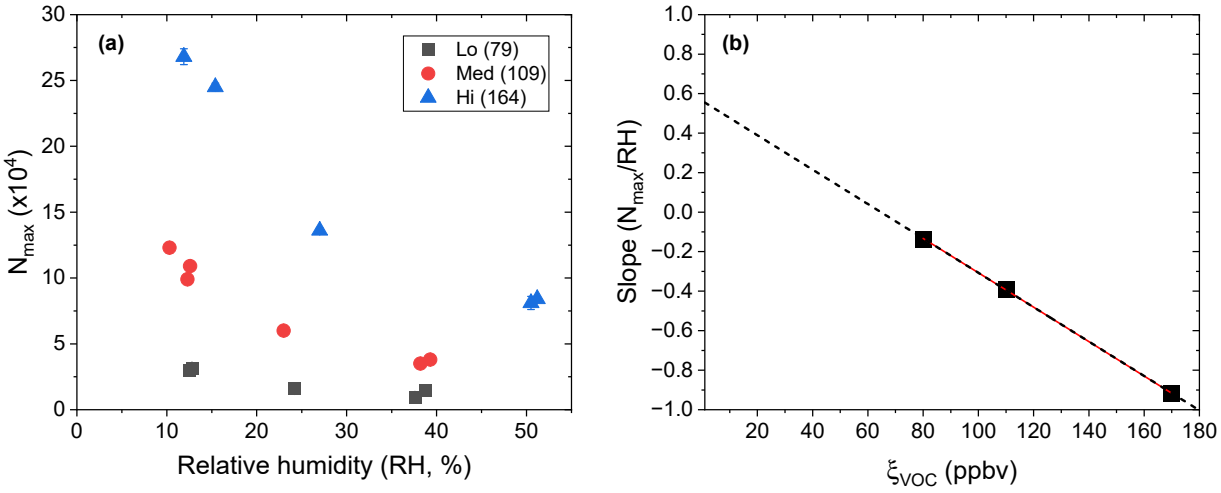

Figure 5. (**a**) Trends in NPF for β-pinene ozonolysis as a function of relative humidity. (**b**) Slope humidity trends in (**a**) as a function of ξ_{VOC}. Here, N_{max} data (**a**) were extrapolated from Emanuelsson et al. [11], and the slope at each ξ_{VOC} (**b**) was determined by linear fits to the Emanuelsson data from 10 to 30% RH.

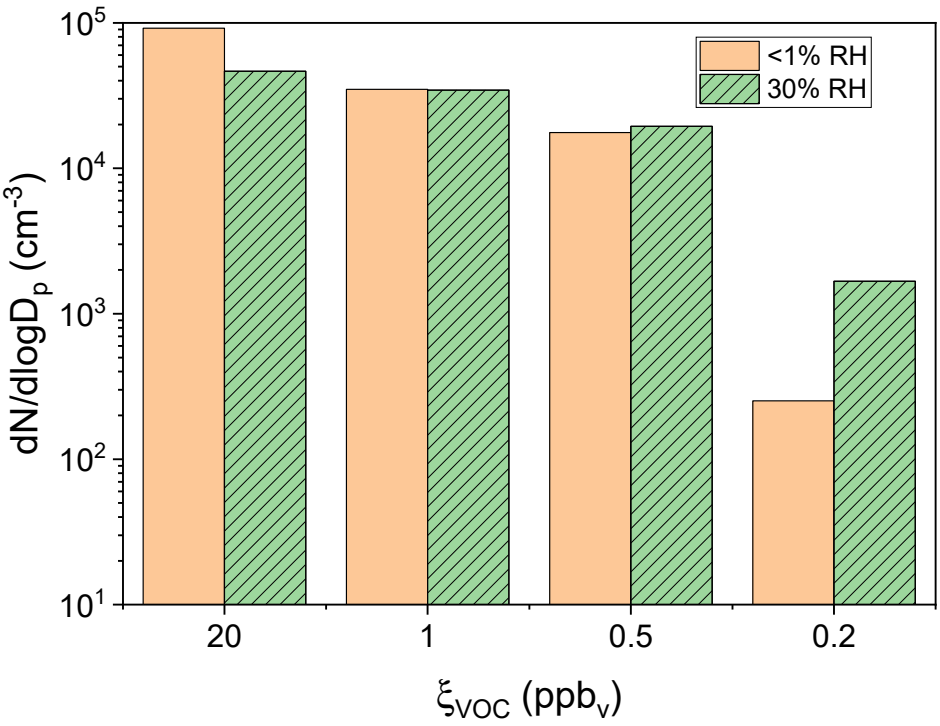

Figure 6. NPF from dark ozonolysis of β-pinene at two levels of RH and as a function of ξ_{VOC}. ξ_{O3} = 500 (±10) ppb_v.

Kirkby et al. [31] studied nucleation rates of pure biogenic particles from ozonolysis of α-pinene at atmospherically relevant mixing ratios of <1 ppb_v α-pinene and 30–35 ppb_v O_3. They found that ion induced nucleation (IIN) rates exceeded neutral nucleation rates by more than an order of magnitude across all humidities studied (5–80%). Furthermore, they showed that, while IIN rates were only modestly enhanced as a function of increasing RH (factor of 2), neutral nucleation rates exhibited a strong positive correlation (factor of 100) with RH. Their studies were conducted under pristine conditions representative of the pre-industrial environment, which included very low concentrations of sulfuric acid. The importance of such sulfuric-acid-free clusters for NPF is also suggested from field measurements [32,33]. As neutral nucleation is expected to dominate in the lower

troposphere, the results of Kirby et al. [31] support our observation that, at low ξ_{VOC}, RH enhances NPF. We cannot speculate whether at low ξ_{VOC} a reduced RH suppresses NPF or high RH enhances NPF, but our results demonstrate the importance of understanding that different RHs at particle genesis can have an effect on NPF; this information can help better predict SOA formation behavior in the atmosphere. Based on our work, contrary to general conclusions drawn from experiments conducted at high RH and high ξ_{VOC}, at low ξ_{VOC}, an elevated RH results in enhanced NPF relative to dry conditions (for the case of α- and β-pinene). It should be noted that while we were not able to quantify the sulfuric acid concentration in our chamber, we expect it would be very low, as the air is extensively filtered and scrubbed. It is apparent, therefore, that the impact of RH on pure organic NPF in pristine environments depends on the absolute mixing ratios of reactants.

3.2. Rates of NPF with Varying RH

Rates of organic NPF were measured using the extracted particle number data from the ELPI+. The ELPI+ outputs a particle distribution over 14 size bins (ranging from 6 nm–15 µm), and the total particle number (# cm^{-3} s^{-1}) was used to produce a 'particle growth curve' (total particle number sampled at 1 Hz for 20 min). Ozonolysis of α-pinene (ξ_{VOC} = 10 ppb_v) was performed for a series of elevated RHs (8, 16, 30, and 60% RH, n = 1 for each). For each RH, the curve (Figure 7, particle number cm^{-3} s^{-1}) was normalized, and the slope of the linear portion was used to quantitatively determine the effect of RH on the rate of NPF at atmospherically relevant ξ_{VOC}.

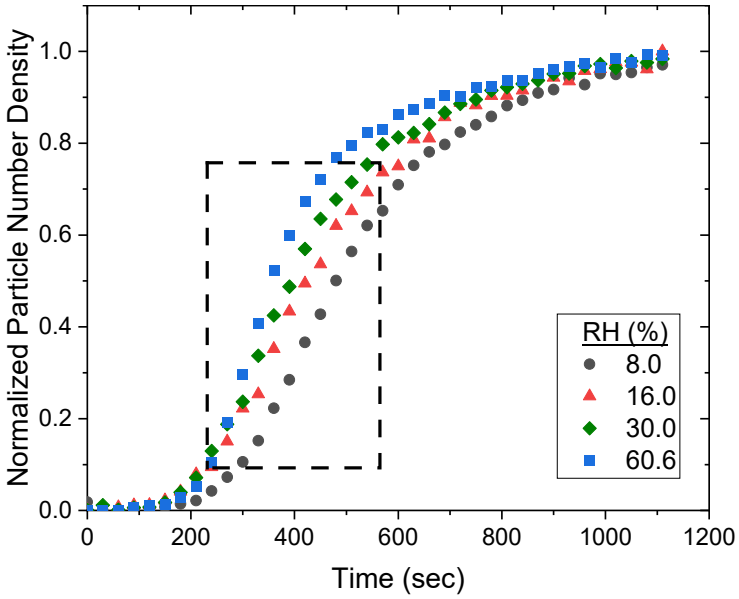

Figure 7. Normalized particle growth curves for ozonolysis of α-pinene at four RHs. The dashed box highlights the linear portion of each curve, where the normalized rate of formation (slope) was extracted for quantitative comparison.

For the ozonolysis of α-pinene (ξ_{VOC} = 10 ppb_v) under increasing RH, there is consequently an increase in the normalized rate of NPF (J_{NR}). Table 4 outlines the rate results with respect to RH. At a ξ_{VOC} of 10 ppb_v, there is a 31.9% increase in J_{NR} at 60% RH compared to J_{NR} at 8% RH. Therefore, the presence of water yields an effect on the rate of particle formation at particle genesis of SOA formed from atmospherically relevant ξ_{VOC}. To probe this idea further, we also observed that NPF enhancements (ΔN_{max} calculated in accord with Equation (1) for the different RH conditions studied) correlated with increased J_{NR} at elevated RH (Figure 8). When performing a log-log plot of the enhancement of NPF under humid conditions with respect to J_{NR}, the rate (slope) is 11.2, suggesting a very small increase in J_{NR} results in a dramatic enhancement in NPF.

Table 4. Rate of NPF results corresponding to particle genesis at increasing levels of RH. Rate of particle formation (cm^{-3} s^{-1}) was normalized for each RH for comparison.

Experiment	RH (%)	Normalized Rate of NPF (s^{-1})
$aP_{10}RH_8$	8.0	4.96×10^{-3}
$aP_{10}RH_{16}$	16.0	5.16×10^{-3}
$aP_{10}RH_{30}$	30.0	5.72×10^{-3}
$aP_{10}RH_{60}$	60.6	6.54×10^{-3}

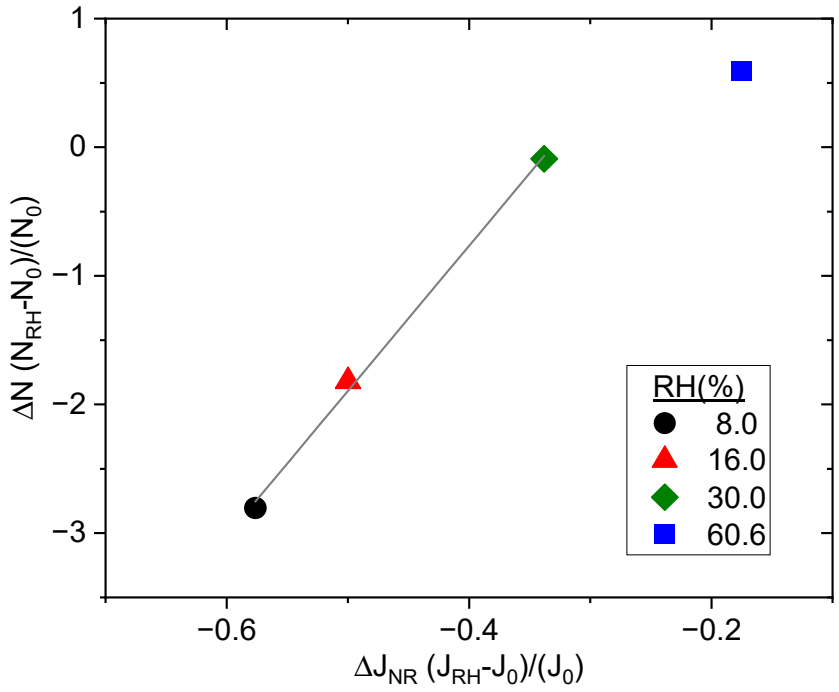

Figure 8. Correlation of ΔN with ΔJ_{NR} for 10 ppb_v α-pinene ozonolysis as a function of RH. ξ_{O3} = 500 ppb_v. Note log scales.

4. Discussion

Secondary organic aerosols constitute a major fraction of the atmospheric organic aerosol burden. Yet, our understanding of factors impacting organic NPF remains unclear. Contradictory reports have appeared in the literature with respect to the impact of RH on NPF, with some reporting significant reductions in NPF at elevated RH, while others report modest enhancements. We undertook a series of experiments to study the impact of RH on NPF from the dark ozonolysis of α-pinene at mixing ratios approaching atmospherically relevant levels and extending to the higher levels typically used in laboratory chamber studies. We found that the impact of RH on NPF depends on the ξ_{VOC}, with significant enhancements observed at lower ξ_{VOC}.

In a pristine environment, the gas phase concentration of these products can grow until supersaturation is exceeded, at which point new organic particles may form by homogeneous nucleation. If, on the other hand, there already exists a population of seed aerosol, then the products can partition to the condensed phase, adding to the total mass of organic aerosol. One can, therefore, envision a dynamic competition between nucleation and partitioning that depends on the rate of product formation, saturation vapor pressure of oxidation products, and mass of existing seed aerosol to promote partitioning.

Partitioning of organic vapors to the condensed phase has been described extensively in the literature [27,28,30,34,35]. Briefly, the partition coefficient (K_p) quantifies the distributions of oxidation products between the gas and condensed phases. K_p depends, in part,

directly on the weight fraction of the aerosol that comprises absorbing organic material phase (f_{om}) and inversely on the average molecular weight of the absorbing particle phase ($\bar{MW}$). All other factors being equal, adding water to the organic phase uniformly reduces $\bar{MW}$, thereby increasing K_p and the corresponding C_{SOA}. This outcome is supported qualitatively in Figure 4, where we measure an approximate 30% increase in C_{SOA} at a RH = 60% relative to dry conditions. Interestingly, however, we see a much greater increase in C_{SOA} at elevated RH and lower ξ_{VOC}. We hypothesize that the "additional" enhancement is likely due to the increased rate of NPF observed under those conditions. That is, not only do we observe greater partitioning under humid conditions, but we also generate a greater number of particles (and hence C_{SOA}) to which partitioning can occur.

The mechanism(s) by which NPF is enhanced under humid conditions at lower ξ_{VOC} remain(s) unclear. According to the volatility basis set (VBS) model [36], partitioning of gas phase products is governed by the balance between C_{SOA} (the partition sink) and $C^*(T)$ (the effective saturation concentration of a product at temperature T). When the two are equal, the VBS model predicts that the product resides equally in the gas and particle phases. For saturation concentrations 10x greater or smaller than C_{SOA}, those products are assumed to fully partition or remain in the gas phase, respectively. This suggests that as C_{SOA} increases, progressively higher volatility products will partition effectively to the particle phase. Of course, in the absence of any seed aerosol (i.e., $C_{SOA} = 0$), no partitioning can occur, and the gas-phase concentration of an oxidation product can increase until it exceeds $C^*(T)$, at which point nucleation of the saturated vapor phase can occur to reestablish equilibrium. In a pristine environment, where C_{SOA} initially is zero, nucleation will begin once $C_g > C^*(T)$. Emanuelsson et al. [11] found that the volatility of products generated under humid conditions was higher for experiments utilizing greater ξ_{VOC} (164 and 109 ppb_v) but inverted (i.e., humid-generated aerosol was less volatile) for the lowest ξ_{VOC} studied (79 ppb_v). If oxidation products are less volatile under humid conditions (i.e., lower $C^*(T)$) at low ξ_{VOC}, then one could expect that supersaturation is more easily achieved, resulting in increased rates of NPF.

New particle formation will continue to dominate until $C_{SOA} \gtrsim C^*(T)$. At this point, C_g will be effectively depleted and NPF disfavored relative to SOA growth. At higher ξ_{VOC}, C_{SOA} rapidly reaches levels approaching $C^*(T)$ of anticipated products [36] of α-pinene oxidation, effectively maintaining C_g below levels of supersaturation and preventing homogeneous nucleation to form new particles. Furthermore, at the higher ξ_{VOC}, products are more volatile and therefore less likely to participate in NPF. The above hypothesis would predict that particle size growth rates would be greater at higher ξ_{VOC}, where partitioning is favored. On the contrary, at low ξ_{VOC}, where C_g is quickly depleted upon NPF and $C_{SOA} < C^*(T)$, we would predict much slower particle growth (due to decreased partitioning). Figure 9 shows the normalized rate of change in GMD as a function of RH in the first 5 min of aerosol formation. We see that the particle size increases almost three times faster at 8% RH than at 60% RH. Keeping in mind that ξ_{VOC} and ξ_{O3} were the same for all experiments, then clearly the enhanced growth rate at 8% cannot be due to enhanced partitioning due to water uptake in the particles. Therefore, it is likely that the greater rate of NPF at higher RH depletes gas phase concentrations before a significant C_{SOA} is developed, thereby limiting partitioning and subsequent particle growth.

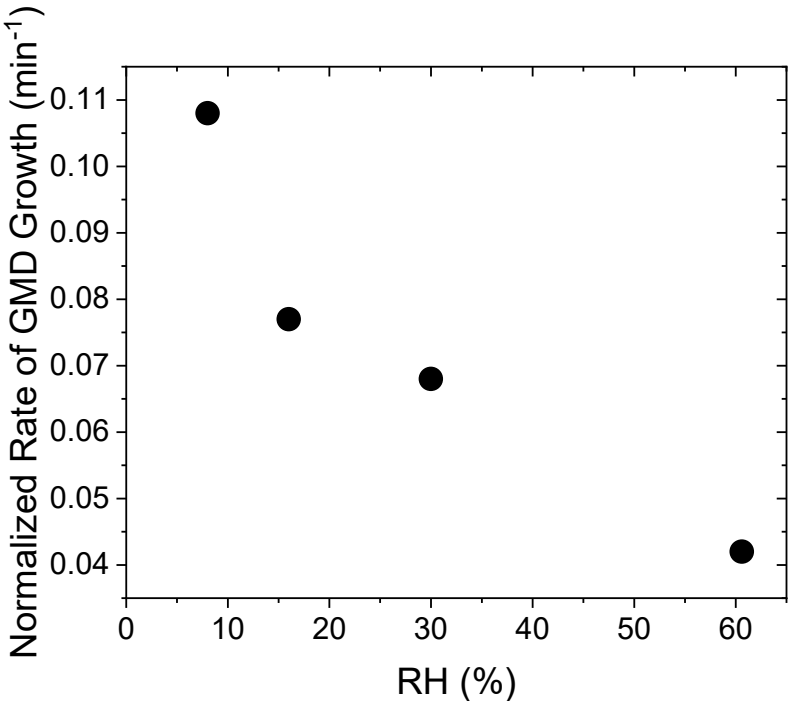

Figure 9. Normalized rate of GMD growth for 10-ppb$_v$ α-pinene aerosol as a function of RH.

Ultimately, we hypothesize that enhanced NPF is due to the combined set of circumstances of lower C_{SOA} and greater rate of production and subsequent nucleation of oxidized products under humid conditions. If our hypothesis is correct, then it follows that analogous behavior would be observed for other monoterpene SOA precursors. Of course, as the volatility distribution of oxidation products will vary with SOA precursor, the ξ_{VOC} at which NPF enhancement is observed under humid conditions will also vary.

5. Conclusions

In the case of dark ozonolysis of α- and β-pinene, we have demonstrated that SOA particle formation and growth depends dramatically upon RH as a function of ξ_{VOC}. When considering ξ_{VOCs} of atmospheric relevance, elevated RH enhances NPF (nucleation) at the expense of particle growth (partitioning). We were able to show, in confirmation of the previous literature reports, that the effect is reversed at higher ξ_{VOCs} typical of laboratory studies. In that case, the rapid development of a significant SOA mass loading, in combination with uptake of water by the particles, results in particle numbers being decreased and SOA mass being increased at high humidity. While we have not been able to unambiguously identify the mechanisms responsible for this outcome for α-pinene, our results suggest that this behavior will also be exhibited by other monoterpene SOA precursors. If confirmed for other SOA precursors, these results suggest that current model estimates underestimate NPF at atmospherically relevant conditions. In fact, the approximate eight-fold enhancement in NPF could serve to significantly narrow the gap between modeled and experimentally measured particle concentrations in the atmosphere.

Author Contributions: C.N.S. carried out experiments for the NPF of α-pinene. A.C.F. carried out rate of particle formation experiments for α-pinene and NPF experiments with β-pinene. G.A.P. supervised all laboratory activities. All authors have read and agreed to the published version of the manuscript.

Funding: This material is based upon work supported by the National Science Foundation under grant no. CHE-1709751.

Institutional Review Board Statement: Not applicable.

Informed Consent Statement: Not applicable.

Data Availability Statement: Data is contained within the article.

Conflicts of Interest: The authors declare no conflict of interest.

References

1. Kanakidou, M.; Seinfeld, J.H.; Pandis, S.N.; Barnes, I.; Dentener, F.J.; Facchini, M.C.; Van Dingenen, R.; Ervens, B.; Nenes, A.; Nielsen, C.J.; et al. Organic aerosol and global climate modelling: A review. *Atmos. Chem. Phys.* **2005**, *5*, 1053–1123. [CrossRef]
2. Ling, Z.H.; Wu, L.Q.; Wang, Y.H.; Shao, M.; Wang, X.M.; Huang, W.W. Roles of semivolatile and intermediate-volatility organic compounds in secondary organic aerosol formation and its implication: A review. *J. Environ. Sci.* **2022**, *114*, 259–285. [CrossRef]
3. Spracklen, D.V.; Carslaw, K.S.; Kulmala, M.; Kerminen, V.M.; Sihto, S.L.; Riipinen, I.; Merikanto, J.; Mann, G.W.; Chipperfield, M.P.; Wiedensohler, A.; et al. Contribution of particle formation to global cloud condensation nuclei concentrations. *Geophys. Res. Lett.* **2008**, *35*, L06808. [CrossRef]
4. Artaxo, P.; Hansson, H.C.; Andreae, M.O.; Back, J.; Alves, E.G.; Barbosa, H.M.J.; Bender, F.; Bourtsoukidis, E.; Carbone, S.; Chi, J.S.; et al. Tropical and Boreal Forest Atmosphere Interactions: A Review. *Tellus B* **2022**, *74*, 24–163. [CrossRef]
5. Hakola, H.; Hellen, H.; Hemmila, M.; Rinne, J.; Kulmala, M. In situ measurements of volatile organic compounds in a boreal forest. *Atmos. Chem. Phys.* **2012**, *12*, 11665–11678. [CrossRef]
6. Huang, W.; Li, H.Y.; Sarnela, N.; Heikkinen, L.; Tham, Y.J.; Mikkila, J.; Thomas, S.J.; Donahue, N.M.; Kulmala, M.; Bianchi, F. Measurement report: Molecular composition and volatility of gaseous organic compounds in a boreal forest—From volatile organic compounds to highly oxygenated organic molecules. *Atmos. Chem. Phys.* **2021**, *21*, 8961–8977. [CrossRef]
7. Maki, M.; Aalto, J.; Hellen, H.; Pihlatie, M.; Back, J. Interannual and Seasonal Dynamics of Volatile Organic Compound Fluxes From the Boreal Forest Floor. *Front. Plant Sci.* **2019**, *10*, 191. [CrossRef]
8. Yanez-Serrano, A.M.; Nolscher, A.C.; Bourtsoukidis, E.; Alves, E.G.; Ganzeveld, L.; Bonn, B.; Wolff, S.; Sa, M.; Yamasoe, M.; Williams, J.; et al. Monoterpene chemical speciation in a tropical rainforest: Variation with season, height, and time of day at the Amazon Tall Tower Observatory (ATTO). *Atmos. Chem. Phys.* **2018**, *18*, 3403–3418. [CrossRef]
9. Porter, W.C.; Jimenez, J.L.; Barsanti, K.C. Quantifying Atmospheric Parameter Ranges for Ambient Secondary Organic Aerosol Formation. *ACS Earth Space Chem.* **2021**, *5*, 2380–2397. [CrossRef]
10. Caudillo, L.; Rorup, B.; Heinritzi, M.; Marie, G.; Simon, M.; Wagner, A.C.; Muller, T.; Granzin, M.; Amorim, A.; Ataei, F.; et al. Chemical composition of nanoparticles from alpha-pinene nucleation and the influence of isoprene and relative humidity at low temperature. *Atmos. Chem. Phys.* **2021**, *21*, 17099–17114. [CrossRef]
11. Emanuelsson, E.U.; Watne, A.K.; Lutz, A.; Ljungstrom, E.; Hallquist, M. Influence of Humidity, Temperature, and Radicals on the Formation and Thermal Properties of Secondary Organic Aerosol (SOA) from Ozonolysis of beta-Pinene. *J. Phys. Chem. A* **2013**, *117*, 10346–10358. [CrossRef] [PubMed]
12. Jonsson, A.M.; Hallquist, M.; Ljungstrom, E. Impact of humidity on the ozone initiated oxidation of limonene, Delta(3)-carene, and alpha-pinene. *Environ. Sci. Technol.* **2006**, *40*, 188–194. [CrossRef] [PubMed]
13. Yu, K.P.; Lin, C.C.; Yang, S.C.; Zhao, P. Enhancement effect of relative humidity on the formation and regional respiratory deposition of secondary organic aerosol. *J. Hazard. Mater.* **2011**, *191*, 94–102. [CrossRef] [PubMed]
14. Hamed, A.; Korhonen, H.; Sihto, S.L.; Joutsensaari, J.; Jarvinen, H.; Petaja, T.; Arnold, F.; Nieminen, T.; Kulmala, M.; Smith, J.N.; et al. The role of relative humidity in continental new particle formation. *J. Geophys. Res.-Atmos.* **2011**, *116*, D03202. [CrossRef]
15. Li, J.J.; Wang, G.H.; Cao, J.J.; Wang, X.M.; Zhang, R.J. Observation of biogenic secondary organic aerosols in the atmosphere of a mountain site in central China: Temperature and relative humidity effects. *Atmos. Chem. Phys.* **2013**, *13*, 11535–11549. [CrossRef]
16. Li, X.X.; Chee, S.; Hao, J.M.; Abbatt, J.P.D.; Jiang, J.K.; Smith, J.N. Relative humidity effect on the formation of highly oxidized molecules and new particles during monoterpene oxidation. *Atmos. Chem. Phys.* **2019**, *19*, 1555–1570. [CrossRef]
17. Liang, L.L.; Engling, G.; Cheng, Y.; Zhang, X.Y.; Sun, J.Y.; Xu, W.Y.; Liu, C.; Zhang, G.; Xu, H.; Liu, X.Y.; et al. Influence of High Relative Humidity on Secondary Organic Carbon: Observations at a Background Site in East China. *J. Meteorol. Res.-Prc.* **2019**, *33*, 905–913. [CrossRef]
18. von Hessberg, C.; von Hessberg, P.; Poschl, U.; Bilde, M.; Nielsen, O.J.; Moortgat, G.K. Temperature and humidity dependence of secondary organic aerosol yield from the ozonolysis of beta-pinene. *Atmos. Chem. Phys.* **2009**, *9*, 3583–3599. [CrossRef]
19. Zhao, Z.X.; Le, C.; Xu, Q.; Peng, W.H.; Jiang, H.H.; Lin, Y.H.; Cocker, D.R.; Zhang, H.F. Compositional Evolution of Secondary Organic Aerosol as Temperature and Relative Humidity Cycle in Atmospherically Relevant Ranges. *ACS Earth Space Chem.* **2019**, *3*, 2549–2558. [CrossRef]
20. Bonn, B.; Moortgat, G.K. New particle formation during alpha- and beta-pinene oxidation by O-3, OH and NO3, and the influence of water vapour: Particle size distribution studies. *Atmos. Chem. Phys.* **2002**, *2*, 183–196. [CrossRef]
21. Bonn, B.; Schuster, G.; Moortgat, G.K. Influence of water vapor on the process of new particle formation during monoterpene ozonolysis. *J. Phys. Chem. A* **2002**, *106*, 2869–2881. [CrossRef]
22. Geddes, S.; Nichols, B.; Todd, K.; Zahardis, J.; Petrucci, G.A. Near-infrared laser desorption/ionization aerosol mass spectrometry for measuring organic aerosol at atmospherically relevant aerosol mass loadings. *Atmos. Meas. Tech.* **2010**, *3*, 1175–1183. [CrossRef]
23. Presto, A.A.; Huff Hartz, K.E.; Donahue, N.M. Secondary Organic Aerosol Production from Terpene Ozonolysis. 2. Effect of NOx Concentration. *Environ. Sci. Technol.* **2005**, *39*, 7046–7054. [CrossRef] [PubMed]

24. Flueckiger, A.; Petrucci, G.A. Methodological advances to improve repeatability of SOA generation in enivronmental chambers. *Atmos. Meas. Tech.* **2022**. *under review*.
25. Jonsson, A.M.; Hallquist, M.; Ljungstrom, E. Influence of OH scavenger on the water effect on secondary organic aerosol formation from ozonolysis of limonene, Delta(3)-carene, and alpha-pinene. *Environ. Sci. Technol.* **2008**, *42*, 5938–5944. [CrossRef]
26. Kristensen, K.; Jensen, L.N.; Quelever, L.L.J.; Christiansen, S.; Rosati, B.; Elm, J.; Teiwes, R.; Pedersen, H.B.; Glasius, M.; Ehn, M.; et al. The Aarhus Chamber Campaign on Highly Oxygenated Organic Molecules and Aerosols (ACCHA): Particle formation, organic acids, and dimer esters from alpha-pinene ozonolysis at different temperatures. *Atmos. Chem. Phys.* **2020**, *20*, 12549–12567. [CrossRef]
27. Seinfeld, J.H.; Erdakos, G.B.; Asher, W.E.; Pankow, J.F. Modeling the formation of secondary organic aerosol (SOA). 2. The predicted effects of relative humidity on aerosol formation in the alpha-pinene-, beta-pinene-, sabinene-, Delta(3)-Carene-, and cyclohexene-ozone systems. *Environ. Sci. Technol.* **2001**, *35*, 1806–1817. [CrossRef]
28. Pankow, J.F.; Marks, M.C.; Barsanti, K.C.; Mahmud, A.; Asher, W.E.; Li, J.Y.; Ying, Q.; Jathar, S.H.; Kleeman, M.J. Molecular view modeling of atmospheric organic particulate matter: Incorporating molecular structure and co-condensation of water. *Atmos. Environ.* **2015**, *122*, 400–408. [CrossRef]
29. Prisle, N.L.; Engelhart, G.J.; Bilde, M.; Donahue, N.M. Humidity influence on gas-particle phase partitioning of alpha-pinene + O-3 secondary organic aerosol. *Geophys. Res. Lett.* **2010**, *37*, L01802. [CrossRef]
30. Qin, Y.; Ye, J.; Ohno, P.; Zhai, J.; Han, Y.; Liu, P.; Wang, J.; Zaveri, R.A.; Martin, S.T. Humidity Dependence of the Condensational Growth of α-Pinene Secondary Organic Aerosol Particles. *Environ. Sci. Technol.* **2021**, *55*, 14360–14369. [CrossRef]
31. Kirkby, J.; Duplissy, J.; Sengupta, K.; Frege, C.; Gordon, H.; Williamson, C.; Heinritzi, M.; Simon, M.; Yan, C.; Almeida, J.; et al. Ion-induced nucleation of pure biogenic particles. *Nature* **2016**, *533*, 521–526. [CrossRef] [PubMed]
32. Bianchi, F.; Junninen, H.; Bigi, A.; Sinclair, V.A.; Dada, L.; Hoyle, C.R.; Zha, Q.; Yao, L.; Ahonen, L.R.; Bonasoni, P.; et al. Biogenic particles formed in the Himalaya as an important source of free tropospheric aerosols. *Nat. Geosci.* **2021**, *14*, 4–9. [CrossRef]
33. Bianchi, F.; Trostl, J.; Junninen, H.; Frege, C.; Henne, S.; Hoyle, C.R.; Molteni, U.; Herrmann, E.; Adamov, A.; Bukowiecki, N.; et al. New particle formation in the free troposphere: A question of chemistry and timing. *Science* **2016**, *352*, 1109–1112. [CrossRef] [PubMed]
34. Jathar, S.H.; Mahmud, A.; Barsanti, K.C.; Asher, W.E.; Pankow, J.F.; Kleeman, M.J. Water uptake by organic aerosol and its influence on gas/particle partitioning of secondary orga nic aerosol in the United States. *Atmos. Environ.* **2016**, *129*, 142–154. [CrossRef]
35. Pankow, J.F. Organic particulate material levels in the atmosphere: Conditions favoring sensitivity to varying relative humidity and temperature. *Proc. Natl. Acad. Sci. USA* **2010**, *107*, 6682–6686. [CrossRef]
36. Stolzenburg, D.; Wang, M.Y.; Schervish, M.; Donahue, N.M. Tutorial: Dynamic organic growth modeling with a volatility basis set. *J. Aerosol. Sci.* **2022**, *166*, 106063. [CrossRef]